Kent Academic Repository

Rehal, Reg, Gaffney, Piers R. J., Hubbard, Alasdair T. M., Barker, Robert D and Harvey, Richard D. (2019) *The pH-dependence of lipid-mediated antimicrobial peptide resistance in a model Staphylococcal plasma membrane: a two-for-one mechanism of epithelial defence circumvention.* European Journal of Pharmaceutic Sciences, 128 . pp. 43-53. ISSN 0928-0987.

The pH-dependence of lipid-mediated antimicrobial peptide resistance in a model Staphylococcal plasma membrane: a two-for-one mechanism of epithelial defence circumvention.

Reg Rehal[a], Piers R. J. Gaffney[b], Alasdair T. M. Hubbard[c,1], Robert D. Barker[d,2], Richard D. Harvey[a,3]*

[a]School of Cancer and Pharmaceutical Sciences, King's College London, London, UK.

[b]Department of Chemical Engineering, Imperial College, London, UK.

[c]Infection and Immunity Research Centre, St George's, University of London, London, UK

[d]Institut Laue Langevin, Grenoble, France

[1]Liverpool School of Tropical Medicine, Pembroke Place, Liverpool, UK.

[2]School of Physical Sciences, University of Kent, Canterbury, UK.

[3]Institut für Pharmazie, Martin-Luther-Universität Halle-Wittenberg, Halle (Saale), Germany.

*Corresponding author: tel. +49 3455525215, e-mail richard.harvey@pharmazie.uni-halle.de

Abstract

The mechanisms of membrane defence by lysylphosphatidylglycerol (LPG), were investigated using synthetic biomimetic mono- and bilayer models of methicillin resistant *S. aureus* ST239 TW, based on its lipid composition in both pH 7.4 (28% LPG) and pH 5.5 (51% LPG) cultures. These models incorporated a stable synthetic analogue of LPG (3adLPG) to facilitate long-duration biophysical studies, which were previously limited by the lability native LPG. Both increased 3adLPG content and full headgroup ionization at pH 5.5, increased bilayer order and dampened overall charge, via the formation of neutral ion pairs with anionic lipids. Ion pair formation in air/liquid interface lipid monolayers elicited a significant condensing effect, which correlated with the inhibition of subphase-injected magainin 2 F5W partitioning. In fluid phase lipid vesicles, increasing the proportion of 3adLPG from 28 to 51 mol% completely inhibited the adoption of the membrane-active α-helical conformation of the peptide, without the need for full headgroup ionization. Neutron reflectivity measurements performed on biomimetic PG/3adLPG fluid floating bilayers, showed a significant ordering effect of mild acidity on a bilayer containing 30 mol% 3adLPG, whilst peptide binding/partitioning was only fully inhibited in a bilayer with 55 mol% 3adLPG at pH 5.5. These findings are discussed with respect to the roles of LPG in resistance to human epithelial defences in *S. aureus* and the continued evolution of this opportunistic pathogen's virulence.

Keywords

1. Introduction

The ability of commensal bacteria to survive on and colonize human body surfaces, such as the skin or various mucosa, is in part facilitated by intrinsic factors which impart resistance to non-specific defences expressed by their host, such as localized acidity or antimicrobial peptides (AMPs) (Hornef, et al. 2005). Often commensal organisms themselves secrete antimicrobial substances, such as fatty acids, bacteriocins or lantibiotics, which serve to discourage competition and reinforce the hostile environment produced by the host's innate immune defences (Nakatsuji, et al. 2017, Hakansson, et al. 2018). In the case of the opportunistic pathogen *Staphylococcus aureus*, a common resident of the nasopharyngeal mucosa and the skin (Wertheim, et al. 2005), it is also a target for topically applied therapeutic antimicrobials designed to treat or prevent infections, especially in healthcare settings. Although such clinical interventions are for the most part successful, there is evidence that some *S. aureus* strains develop adaptations which enable it to colonize body surfaces resulting in the increased incidence of resistance to important antibiotics of last resort such as daptomycin and vancomycin (Mishra, et al. 2009, Bayer, et al. 2016, Chen, et al. 2018). This exemplifies the role of evolution driving the increased virulence of an opportunistic pathogen through an enhancement of its intrinsic mechanisms for host epithelial defence circumvention (Alekshun and Levy 2006, Dobson, et al. 2013).

One of the most important mediators of resistance to innate immune defences in *S. aureus* is the phospholipid, lysylphosphatidylglycerol (LPG). LPG is a major component of the bacterium's plasma membrane and has been shown to play a role in resistance to

host cationic AMPs (Roy 2009). The LPG headgroup has three ionizable moieties (figure 1A), the phosphate, with a pK_a of ~3, the epsilon amine with a pK_a of ~10 and the alpha amine with a pK_a of ~6.5 (Tocanne, et al. 1974), making it predominantly zwitterionic at neutral pH and cationic in mildly acidic conditions. The biosynthesis of LPG is catalysed by the membrane-intrinsic lysyl transferase MprF, which increases in expression in *S. aureus* upon exposure to antimicrobial peptides (Li, et al. 2007). Resistance to AMP is therefore thought to be conferred by a dampening of the anionic charge on the plasma membrane caused by increasing amounts of LPG, leading to reduced affinity for the AMP and therefore attenuation of their membrane-lytic effect (Peschel, et al. 2001, Ernst and Peschel 2011). Ion-pairing between LPG and the anionic lipids, phosphatidylglycerol (PG) or cardiolipin (CL), which are the only other major phospholipids in the *S. aureus* membrane, may further reduce AMP penetration by increasing membrane viscosity (Roy 2009, Rehal, et al. 2017).
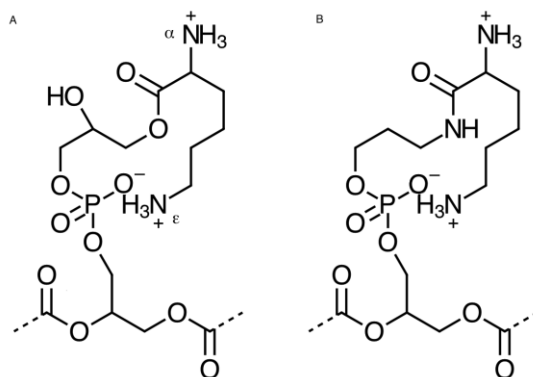
Figure 1. Headgroup structures of A) native lysyl-phosphatidylglycerol and B) synthetic 3-aza-dehydroxy lysyl-phosphatidylglycerol, showing the various ionisable groups in the conformation proposed by El Mashak and Tocanne (El Mashak and Tocanne 1979).

To date, most of the evidence for the role of LPG in defending *S. aureus* against membrane lytic threats, has come from molecular biology studies rather than mechanistic biophysical investigations, although synthetic LPG has previously been used in model *S. aureus* membranes to study their interaction with AMPs. These biophysical studies have suggested that LPG does not inhibit peptide binding, but only impedes their penetration into lipid bilayers (Kilelee, et al. 2010). However, the proper interpretation of these results is problematic since LPG has a highly labile ester in its headgroup, which is readily hydrolysed at neutral pH (Danner, et al. 2008). In order to prevent the problem of LPG hydrolysis during biophysical investigations into its effect on membrane characteristics and AMP interaction, one approach has been to synthesize a stable analogue, such as lysylphosphatidylethanolamine (LPE), which has been used to examine peptide/membrane interactions in model *S. aureus* bilayers (Cox, et al. 2014). What has hitherto been mostly overlooked, however, is the influence of pH on the behaviour of LPG both as a major component of the *S. aureus* plasma membrane and in facilitating protection against AMP activity. This is especially important since mild acidity has an influence on both the biosynthesis of LPG and its headgroup ionization, two factors which influence the physicochemical behaviour of the lipid as well as membranes when present in significant amounts (Rehal, et al. 2017). LPG biosynthesis is markedly increased by exposure to mildly acidic environments (Gould and Lennarz 1970), and may therefore play a role in the colonization of mammalian mucosa by facilitating acid tolerance (Cotter and Hill 2003), as well as providing a means of resisting AMPs present as innate mucosal defences (Li, et al. 2007), which constitutes a two-for-one mechanism for circumventing those defences. Therefore, when investigating the role of LPG within model membrane

systems attention needs to be paid to the environmental pH, in order to more closely mimic mildly acidic conditions encountered by the bacterium on its host (Washington, et al. 2000, Schreml, et al. 2010) and the natural acidity of the outer leaflet of the bacterial plasma membrane itself (Collins and Hamilton 1976).

In this study we have addressed the above issues by using a synthetic stable analogue of LPG, named 1,2-*O*-dipalmitoyl-3-aza-dehydroxy lysylphosphatidylglycerol (DP3adLPG) (figure 1B) in both fully hydrogenated and chain-deuterated forms, to substitute for native LPG in biophysical investigations. We have chosen model membrane systems whose lipid compositions are based upon those found in a highly virulent strain of methicillin resistant *S. aureus* (MRSA) (Edgeworth, et al. 2007) when cultured at pH 7.4 and at pH 5.5 (Rehal, et al. 2017), in order to examine the effect of both the increased proportion of LPG obtained under mildly acidic conditions, and the influence of bulk pH upon membrane behaviour. In each experiment we have challenged the membrane models with the bilayer-disrupting AMP analogue magainin 2 F5W (Matsuzaki, et al. 1998) in order to assess the nature of the peptide-membrane interaction with increased 3adLPG concentrations as well as at the two pH values. Our initial investigation into the propensity for magainin 2 F5W to penetrate into model membranes was conducted using an *S. aureus* mimetic ternary lipid mixture (3adLPG/PG/CL) in the gel phase to monitor surface pressure changes in monolayers deposited at the air/liquid to demonstrate peptide partitioning (Maget-Dana 1999), before determining the degree of peptide folding in the presence of fluid phase *S. aureus* mimetic vesicles, using circular dichroism. Since CL is known to promote the formation of negative membrane curvature (Matsuzaki, et al. 1998), simple binary mixtures of chain-deuterated 3adLPG and PG (in the fluid phase),

were used to form the planar floating bilayers used in our neutron reflectivity studies. The results obtained with all three techniques, clearly showed the importance of 3adLPG content and bulk pH on both the bilayer structure, physical properties and attenuation of AMP activity.

2. Materials and methods

2.1 Materials

Tris(hydroxymethyl)aminomethane (>99.0%), concentrated hydrochloric acid (~38%), concentrated deuterium chloride (99 %D atom), glacial acetic acid, sodium sulphate (>99.0%) and deuterium oxide (99.9 %D atom) were all purchased from Sigma-Aldrich UK, and used as supplied. Ultrapure water (18.2 MΩ.cm) for all experiments was obtained from a Milli-Q 16 Ultrapure water system (Merck Millipore, Billerica, USA). The peptide magainin 2 F5W (GIGKWLHSAKKFGKAFVGEIMNS) was custom synthesized by GenScript (Piscataway, New Jersey, USA) to a purity of >95% and was used as supplied. The phospholipid 1,2-O-dipalmitoyl-sn-glycero-3-phospho-(1'-*rac*-glycerol), sodium salt (DPPG) was purchased from Avanti Polar Lipids (Alabaster, USA), and was converted to the triethylammonium salt by crystallising the conjugate acid from cold acetone using 1.5 eq. HCl, and then filtering off the NaCl and finally crystallising the lipid-triethylammonium salt twice from cold acetone using triethylamine (> 99%) purchased from Sigma-Aldrich, UK. 1,1',2,2'-Tetramyristoyl cardiolipin (TMCL), sodium salt was also purchased from Avanti Polar Lipids (Alabaster, USA) and was used as supplied. The chain-deuterated phospholipids d_{62}1,2-*O*-dipalmitoyl-*sn*-glycero-3-phospho-(1'-*rac*-glycerol),

7

triethylammonium salt (d$_{62}$DPPG), d$_{62}$-1,2-O-dipalmitoyl 3-aza-dehydroxy-lysyl-phosphatidylglycerol, trifluoroacetate salt (d$_{62}$DP3adLPG) and a fully hydrogenated version of DP3adLPG were synthesized at the Institute of Pharmaceutical Science, King's College London (Rehal 2014).

2.2 Synthesis of azo-lysyl-phosphatidylglycerols

The comprehensive synthetic methods of the synthesis of the azo-lysyl-phosphatidylglycerols are described in detail elsewhere (Rehal 2014). Briefly, both deuterated and hydrogenated variants of DP3adLPG, were synthesized by the same synthetic route. 1,2-O-Dipalmitoyl-rac-glycerol was synthesised following the method described by Lok, 1978 (Lok 1978). The 1,2-O-dipalmitoyl-rac-glycerol was then phosphorylated under an inert atmosphere in the presence of dry pyridine with di(2-cyanoethyl) phosphorochloridite, which was synthesised as described by Gaffney $et\ al$. 2001 (Gaffney and Reese 2001). The resulting, phosphite was then oxidised with tert-butyl hydroperoxide to give 1,2-O-dipalmitoyl-3-O-phosphate-rac-glycerol, di(2-cyanoethyl) ester which was purified by crystallisation from cold acetonitrile. Next, 3-aminopropan-1-ol was reacted with N,N'-di-Boc-rac-lysine under an inert atmosphere, in the presence of N-(3-dimethylaminopropyl)-N′-ethylcarbodiimide hydrochloride, a catalytic quantity of 4-(dimethylamino)pyridine and N-hydroxysuccinimide, which yielded 3-N-(N',N''-di-Boc-rac-lysyl)-3-aminopropan-1-ol. 3-N-(N',N''-di-Boc-rac-lysyl)-3-aminopropan-1-ol was then washed with water several times and mixed under and an inert atmosphere with dry pyridine and 1,2-O-dipalmitoyl-3-O-phosphate-rac-glycerol, di(2-cyanoethyl) ester, which was pre-treated for 12 hours under an inert atmosphere with

triethylamine/acetonitrile/dichloromethane 1:1:1 v/v/v. Excess 3-nitro-1H-1,2,4-triazole was then added to the mixture and 2-mesitylenesulfonyl chloride in dry dichloromethane was then added dropwise to the mixture over 30 mins. Fully protected DP3adLPG was then isolated by aqueous washing and normal phase chromatography with an elution gradient of hexane/ethylacetate 0:100 v/v to 100:0 v/v. Fully protected DP3adLPG was then deprotected by treatment for 12 hours under an inert atmosphere with triethylamine/acetonitrile/dichloromethane 1:1:1 v/v/v and then treatment with dichloromethane/trifluoroacetic acid 1:1 v/v for 60 mins. DP3adLPG was finally purified by repeat crystallisation from cold acetone. The identity of each product at each step and the final product was confirmed by NMR, MS and TLC (Rehal 2014).

2.3 The effect of pH on *S. aureus* mimetic mixed monolayers at the air/liquid interface

Ternary mixtures of 5 mg of DPPG/DP3adLPG/TMCL 67:28:5 and 41:51:8 mol/mol/mol, mimicking the MRSA ST239 TW strain (Edgeworth, et al. 2007) lipid composition when cultured at pH 7.4 and 5.5 respectively (Rehal, et al. 2017), were each dissolved in 5 mL of chloroform. To form monolayers, the lipid solutions (~50 µL) were added dropwise to the surface of an aqueous subphase of TRIS–AcOH 1:1 mol/mol adjusted to either pH 5.5 or 7.4 (with concentrated HCl) in a Nima 612D Langmuir trough (NIMA technologies, Coventry, UK). The lipid monolayers were equilibrated for 20 min to ensure evaporation of any residual chloroform. For each lipid mixture on both subphases, isotherms were measured by compressing the monolayers at 23°C with a barrier speed of 25 cm^2/min to

obtain at least 6 measurements per experimental condition. The surface compressional modulus (K^s) for each extract was then calculated using:

$$K^s = -A_{40}\left(\frac{\delta\Pi}{\delta A}\right) \qquad\qquad (1)$$

where, A_{40} is the average molecular area at 40 mN/m, δA is the change in molecular area in Å^2 and $\delta\Pi$ is the change in surface pressure in mN/m. The surface compressional modulus is a quantitative measure of the elasticity of a monolayer as a function of molecular area and provides a quantitative measure of the packing of the lipids at specific surface pressures. A K^s value between 50 and 100 mN/m is considered to be characteristic of the liquid expanded (LE) phase, whereas a value between 100 and 250 mN/m is characteristic of the liquid condensed (LC) phase, the higher the value indicating closer molecular packing (Dynarowicz-Łątka and Hąc-Wydro 2004).

2.4 Peptide interactions with *S. aureus* mimetic mixed monolayers

Monolayers of each of the ternary *S. aureus* mimetic lipid mixtures prepared in section 2.3 were deposited at the air/liquid interface of a custom-made 110 ml polytetrafluoroethane trough with a surface area of the 86.2 cm^2, in order to achieve a stable surface pressure of ~30 mN/m at 23°C. The aqueous subphase consisted of 10 mM Tris-acetate buffer adjusted to either pH 5.5 or 7.4. The deposited monolayers were allowed to stabilize under constant gentle agitation from a magnetic stirring plate placed beneath the trough, the surface pressure being constantly monitored using a PS4 pressure sensor (Nima Technology, Coventry, U.K.) fitted with a chromatography paper

(Whatman 1 Chr) Wilhelmy plate. After achieving a stable measurement of the surface pressure for 200 s, 200 μL of magainin 2 F5W at a concentration of 400 μM, dissolved in the appropriate subphase buffer, was injected underneath the monolayer and the surface pressure was recorded until no further changes were observed. The final concentration of peptide in the subphase was 7.2 μM (giving an approximate lipid/peptide ratio of 1:2), which is above the concentration at which native magainin 2 is sufficiently surface active to achieve maximal interfacial adsorption in various buffer subphases (Bucki, et al. 2004, Lad, et al. 2007). All samples were run in triplicate and data was then analysed by plotting the change in surface pressure ($\Delta\Pi$) against time (*t*) after peptide injection and fitting the curves using a Hill function (Barnes and Chu 2010), in order to calculate the mean time taken for the surface pressure to achieve half the maximal value (*H*) and the mean maximum surface pressure increase (Π_{max}):

$$\Delta\Pi = \frac{\Pi_{max}.t^n}{H^n + t^n} \tag{2}$$

Where, n is the Hill coefficient, which indicates the degree of cooperativity of the peptide binding or penetrating at the monolayer interface. The isotherms produced were also used to calculate the initial rate of surface pressure change by determining the gradient ($\Delta\Pi/t$) of the isotherm during the first 50 seconds after addition of the peptide.

2.5 Circular dichroism studies on the influence of *S. aureus* mimetic vesicles on peptide structure

Vesicles were prepared from ternary mixtures of 5 mg of DPPG/DP3adLPG/TMCL 67:28:5 and 41:51:8 mol/mol/mol lipid mixtures, using the thin film resolvation technique.

The lipids were fully dissolved in ~2 mL of chloroform in a glass vial before the solvent was evaporated under reduced pressure in a vacuum desiccator. The films were briefly put under a nitrogen stream to ensure complete solvent evaporation. The resultant lipid films were dispersed, by vortex mixing, in 2.5 mL of 10 mM Tris-acetate 1:1 mol/mol buffer adjusted to either pH 5.5 or 7.4, to form vesicle dispersions. The vesicles produced were reduced in size using a Soniprobe (Lukas-Dawe Ultrasonics, UK) sonicator fitted with a tapered microtip probe, for 5 min at 10% of its total power output.

Vesicle samples were diluted and mixed with solutions of magainin 2 F5W to give final concentrations of 500 μM lipid and 50 μM peptide in buffers 10 mM Tris-acetate buffers adjusted to maintain either pH 5.5 or 7.4 at 55°C, by the addition of concentrated HCl or NaOH. The vesicle/peptide mixed samples were loaded in to 2 mm pathlength cells prior to circular dichroism (CD) measurements.

Static CD measurement at far-UV (190 nm to 260 nm) was carried out on a Chirascan-Plus spectrometer (Applied Photophysics Ltd, Leatherhead, UK) with a bandwidth of 1 nm scanning at a speed of 3 s time per point at 55°C (to ensure the lipids were in the fluid phase). The recorded CD spectra were subtracted from those obtained from corresponding peptide-free samples. Ellipticity data was then converted from millidegrees to mean residue CD extinction coefficient ($\Delta\epsilon$ in M^{-1} cm^{-1}), smoothed using a Savitsky-Golay filter and analysed for different peptide secondary structure content using the web-based plotting and analysis tool CAPITO (Wiedemann, et al. 2013).

2.6 Neutron reflectivity measurements on *S. aureus* mimetic floating bilayers

Two thoroughly cleaned silicon blocks measuring 38 mm × 70 mm × 10 mm with a single surface for sample deposition polished to a tolerance of 5 Å (Crystran Ltd, Poole, UK), were silanized using 3-(trimethoxysilyl)propyl acrylate monomers (TMPA) (Sigma-Aldrich, Lyon, France) which was subsequently covalently bound to a 1-palmitoyl-2-[16-(acryloyloxy)hexadecanoyl]-*sn*-glycero-3-phosphorylcholine (al-PC) (Avanti Polar Lipids, Alabaster, USA) using the method of Hughes *et al.* (Hughes, et al. 2008). The TMPA and al-PC (collectively known as the self-assembled monolayer - SAM) coated silicon blocks, were mounted in a custom-made plastic sample cell containing a bulk solvent reservoir, prior to being fully characterised on the D17 reflectometer beam line at Institut Laue-Langevin (Grenoble, France) at 55°C (Supplementary Material Table S1). Three solvent contrasts were utilised for the SAM characterization; H_2O which has a coherent scattering length density (SLD; analogous to a neutron refractive index) of -0.56 × 10^{-6} Å^{-2}, D_2O (SLD = 6.38 × 10^{-6} Å^{-2}) and 4-matched water (4MW; a mixture of 34% H_2O and 66% D_2O with an SLD of 4.02 × 10^{-6} Å^{-2}). When required, these solvents were exchanged through the sample cell reservoir using a Knauer Smartline 1050 HPLC pump (Berlin, Germany) at a flow rate of 2 mL/min.

Neutron reflectivity data was collected at two incident angles (0.8°and 3.2°), for 30 min at the lower angle and 50 min at the higher angle (or 12 min and 30 min respectively for D_2O contrasts). The overlapping data from both angles gave a total Q_z range of 8 × 10^{-3} Å^{-1} to 0.32 Å^{-1}, although due to some incoherent scattering Q_z normally reached a maximum of ~0.3 Å^{-1}. The data obtained was analysed by fitting the reflectivity curves with a least squares simplex algorithm using the program RasCal v1.0.0 (ISIS, Rutherford Appleton Laboratory). A four-layer model consisting of surface silicon oxide (SiO_2),

TMPA, al-PC hydrocarbon chains and al-PC headgroups was used to calculate the parameters of layer thickness, layer SLD, % hydration and roughness.

The SAM-coated silicon blocks were used to prepare two floating bilayers of d_{62}DPPG/d_{62}DP3adLPG at molar ratios of 7:3 (to mimic lipid extracts from bacteria cultured at pH 7.4) and 45:55 (to represent bacterial lipid extracts from pH 5.5 culture), using the Langmuir-Blodgett technique to deposit the inner leaflet and the Langmuir-Schafer technique to deposit the outer leaflet, using an automated arm adapted Nima 1212D Langmuir trough (Nima Technologies, Coventry, UK) with a dipping well (Hughes, et al. 2008). The bilayer-coated blocks were then sealed within the sample cells prior to mounting on the D17 beam line.

Neutron reflectivity (NR) measurements were obtained with three solvent contrasts in the following order: H_2O, D_2O, and then silicon matched water (SMW – a mixture of 62% H_2O and 38% D_2O) to contrast match out the silicon substrate (SLD = 2.07×10^{-6} Å^{-2}). All the solvent contrasts were buffered with Tris-acetate buffer adjusted to either pH/pD 7.4 or 5.5 with concentrated HCl or DCl. All data was acquired at 55°C to assess the bilayer characteristics in the lipid liquid crystalline phase in order to mimic the fluid bacterial plasma membrane, firstly in solvents buffered at pH/pD 7.4 and then in the pH/pD 5.5 buffered solvents. After characterization of the two floating bilayers at different pH/pDs, each bilayer had magainin 2 F5W introduced to it by injecting 10 ml of the peptide solution directly into the cell at a concentration of 0.17 µg/ml in the appropriate buffer (giving an approximate lipid to peptide molar ratio of 50:1). After incubation for one hour, excess peptide was flushed away with 10 ml of the appropriate solvent, using the HPLC pump at

a flow rate of 2 mL per minute. The reflectivity measurements were then repeated in the three contrasts, firstly in pH/pD 7.4 solvents and then in pH/pD 5.5 solvents.

After data collection, the fitting of the reflectivity curves followed the same method of the SAM layer characterization with a four-layer model (with each layer characterized according to its SLD, thickness, roughness and % hydration) consisting of a solvent layer (between the SAM and the floating bilayer), the floating bilayer inner leaflet headgroups, the floating bilayer hydrocarbon chains and the outer leaflet headgroups. The parameters were fixed for the headgroups of both leaflets and the same roughness value was used for all the layers within the floating bilayer.

3. Results

3.1 The effect of pH on *S. aureus* mimetic mixed monolayers at the air/liquid interface

The pressure-area isotherms for the pH 7.4 culture mimetic PG/LPG/CL [67:28:5] and the pH 5.5 culture mimetic PG/LPG/CL [41:51:8] lipid mixtures (figure 2) indicate a modest but significant condensing upon acidification of the subphase (table 1). In the isotherms for both lipid mixtures deposited on a pH 7.4 subphase, there is clear evidence of a liquid expanded to liquid condensed (LE/LC) phase transition, the onset of which is between 6 and 7.5 mN/m surface pressure (figure 2). These transitions are less pronounced (although still present) in the isotherms measured on pH 5.5 subphases, which is indicative of the monolayers being more laterally condensed (Miyoshi and Kato 2015). A similar conclusion can be drawn from the decrease in lift-off area observed in both lipid samples when compressed on the pH 5.5 subphase (table 1). The decrease in subphase

pH may facilitate a decrease in lift-off area by promoting the formation of lipid ion pairs between the fully ionized cationic LPG and anionic PG or CL. Such discrete lipid ion-pairs form distinct entities with reduced acyl chain tilt (Schmid, et al. 2018), for which there would be reduced likelihood of steric interaction with other lipids or ion pairs at high molecular areas.
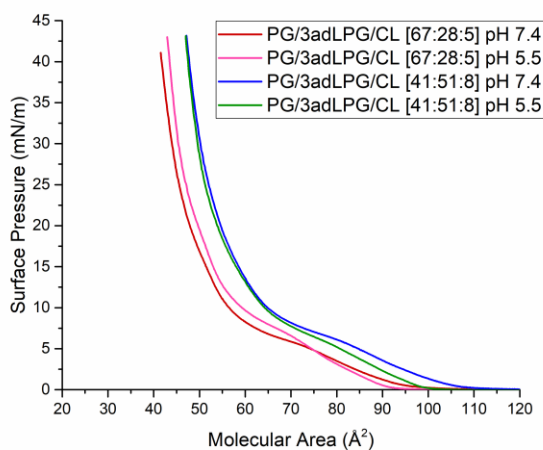
Fig. 2 Mean (n ≥ 6) surface pressure–area isotherms of mixtures of PG/3adLPG/CL, mimicking proportions of membrane lipid obtained from *S. aureus* cultures grown at either pH 7.4 [67:28:5] or pH 5.5 [41:51:8], measured on Tris-acetate buffer subphases adjusted to either pH 7.4 or 5.5 at 23°C.

The surface compressional moduli (K^s) of each of the monolayers examined (table 1) proved to be within the range expected for liquid condensed lipid phases (Dynarowicz-Łątka and Hąc-Wydro 2004) at a surface pressure of 40 mN/m (i.e. >100 mN/m). However, the K^s values calculated for both lipid mixtures are significantly higher on pH 5.5 than they are on pH 7.4 subphases (p<0.05, Mann-Whitney U test). This provides further evidence that the reduction in pH elicits a reduction in monolayer elasticity and

tighter packing between the lipid molecules, likely facilitated by the formation of ion pairs. Interestingly, increasing the proportion of LPG also significantly increases the K^s value (p<0.05, Mann-Whitney U test), without the need to decrease the subphase pH. The increase in mean area per molecule at 40 mN/m (A_{40}) observed in the pH 5.5 culture mimetic monolayers more than likely results from the increase in proportion of 3adLPG, due to its bulky headgroup (figure 1).

Table 1. Mean molecular area, surface compressional modulus and lift-off area for biomimetic mixtures of PG/3adLPG/CL, derived from air/liquid interface monolayers measured on Tris-acetate buffer subphases adjusted to either pH 7.4 or 5.5.

Monolayer composition	Subphase pH	A_{40} (mN/m)	K^s (mN/m)	Lift-off area (Å^2)
PG/3adPG/CL [67:28:5]	7.4	40.8 ± 0.6	210.2 ± 11.3	101
	5.5	43 ± 0.3	268.1 ± 16.3	93
PG/3adPG/CL [41:51:8]	7.4	47 ± 0.5	233.1 ± 4.7	110
	5.5	47.1 ± 0.2	260.1 ± 7.8	100

3.2 Peptide interactions with *S. aureus* mimetic mixed monolayers

The attenuating effects on magainin 2 F5W monolayer partitioning of both increasing the proportion of DP3adLPG within monolayers and increasing its degree of ionization with mild acidity are evident in figure 3. The maximum increase in surface pressure observed after injection of the peptide beneath the pH 7.4 culture mimetic PG/3adLPG/CL [67:28:5] monolayer on the pH 7.4 subphase, is indicative of a strong peptide-lipid interaction leading to partitioning into the monolayer (Maget-Dana 1999). Decreasing the pH of the subphase to 5.5 decreases both the initial rate ($\Delta\Pi/s$) and degree (Π_{max}) of peptide interaction (table 2) and shows that it is not necessary to have cationic lipid predominate within the monolayer, in order to significantly attenuate peptide partitioning ($p<0.05$ Mann-Whitney U test).
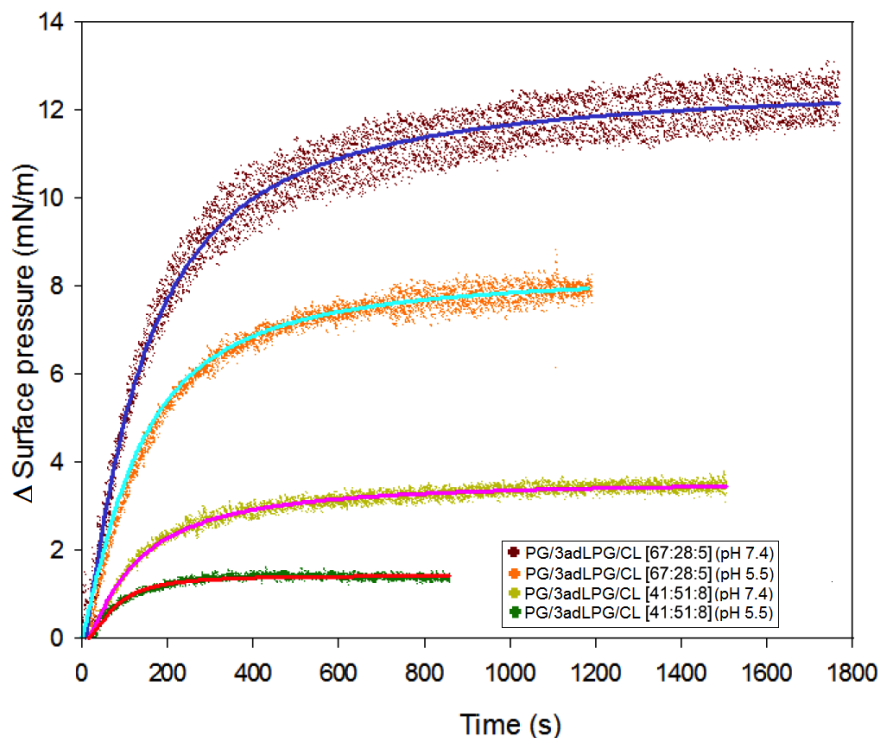
Figure 3. Mean changes in surface pressure over time of monolayers of PG/3adDPPG/CL mixtures in molar ratios of 67:28:5 and 41:51:8 after subphase injection of magainin 2 F5W (lipid/peptide 50:1), on Tris-acetate buffer subphases at pH 7.4 and 5.5 at 23°C. The scatter plots show the experimental data (n=3) and the solid lines represent the fitted Hill plots.

A similar trend was also observed with the pH 5.5 culture mimetic PG/3adLPG/CL [41:51:8] monolayers after introduction of the peptide and lowering of the subphase pH from 7.4 to 5.5. Even without the added effect of a high degree of 3adLPG ionization, the reduction in the proportion of anionic lipids leads to a significant reduction (p<0.05 Mann-Whitney U test) in both the initial rate of peptide interaction and the extent to which it can penetrate into the monolayer. In comparison to with that of low 3adLPG monolayer at pH

7.4, the penetration of the peptide into more ionized monolayer with higher 3adLPG at pH 5.5, is negligible

Table 2. Kinetic parameters obtained from the plots of mean change in surface pressure of the different PG/3adLPG/CL monolayers after subphase injection of magainin 2 F5W. The maximum change in surface pressure (Π_{max}) and time taken to achieve half of the maximum change (H) were determined from the equations for the fitted Hill plots (equation 2). The initial rate of surface pressure change (K) was obtained from the tangent to the Hill plot curves for the first 50 s of measurement.

Monolayer composition	Subphase pH	$K(\Delta\Pi/s)$	Π_{max} (mN/m)	H(s)	n
PG/3adLPG/CL [67:28:5]	7.4	5.14×10^{-2}	13.0 ± 0.9	135.6 ± 10.4	1.2
	5.5	3.72×10^{-2}	8.6 ± 0.4	130.9 ± 8.8	1.2
PG/3adL PG/CL [41:51:8]	7.4	1.75×10^{-2}	3.9 ± 0.6	120.2 ± 12.1	1.2
	5.5	1.43×10^{-2}	1.9 ± 0.2	75.0 ± 6.6	1.5

3.3 Circular dichroism studies on the influence of *S. aureus* mimetic vesicles on peptide structure

The results of the CAPITO analysis of the static CD measurements conducted on magainin 2 F5W mixed with the biomimetic PG/3adLPG/CL vesicles at different pH (figure 4), show the influence of vesicle composition and bulk pH on peptide secondary structure

(table 3). Since the membrane disrupting conformation of magainin 2 F5W predominantly consists of α-helix (Matsuzaki, et al. 1998), it may be assumed that spectra displaying high α-helix content result from penetration of the peptide into the vesicle bilayers. Conversely, spectra indicating little or no α-helix content suggest little peptide penetration into the bilayer.
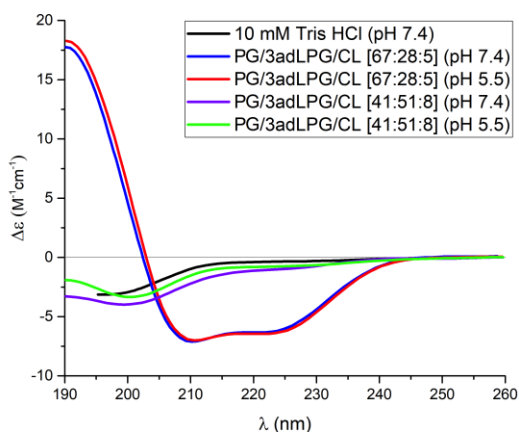
Figure 4. Static circular dichroism spectra for magainin 2 F5W in Tris HCl buffer at pH 7.4, and in the presence of biomimetic PG/3adLPG/CL vesicles in 10 mM Tris-acetate buffers adjusted to either pH 7.4 or 5.5 at 55°C.

At 55°C, when the vesicle bilayer lipids would be expected to be in the fluid phase, the pH 7.4 culture mimetic PG/3adLPG/CL [67:28:5] vesicles appear to be equally vulnerable to attack by magainin 2 F5W at both pH 7.4 and 5.5, since they elicited equivalent high peptide α-helix content (table 3). Increasing the proportion of 3adLPG in the pH 5.5 culture mimetic PG/3adLPG/CL [41:51:8] vesicles, reduces the α-helix content to zero and although there exists a large proportion of unstructured peptide, the CAPITO analysis also suggests that some peptide adopts a β-sheet conformation. Although the proportions

of calculated secondary structures for the peptide mixed with pH 5.5 mimetic vesicles are similar to those obtained from the spectrum for peptide dissolved in buffer alone, the spectra themselves show some differences. This may indicate the formation of some secondary structure due to binding of the peptides to the vesicle surfaces, without the subsequent penetration which would promote the formation of α-helix.

Table 3. Calculated secondary structure content for magainin 2 F5W in Tris HCl buffer and in the presence of biomimetic PG/3adLPG/CL vesicles in Tris-acetate buffers adjusted to pH 7.4 or 5.5, obtained using the web-based CAPITO CD data analysis tool (Wiedemann, et al. 2013).

Sample	Buffer pH	Alpha helix	Beta sheet	Irregular structure
Magainin 2 F5W (buffer only)	7.4	0.03	0.36	0.65
PG/3adPG/CL [67:28:5]	7.4	0.53	0.03	0.24
	5.5	0.57	0.04	0.25
PG/3adPG/CL [41:51:8]	7.4	0	0.24	0.68
	5.5	0	0.29	0.68

3.4 Neutron reflectivity measurements on *S. aureus* mimetic floating bilayers

To improve the resolution of the NR data and thus the accuracy of the fitting, each experimental treatment was measured in at least two different solvent contrasts, the results from which were fitted simultaneously (Supplementary Material figures S2 and S3 for the full set of NR curves and fits for each sample in all of the different contrasts). In order to fit the NR data, the samples were modelled as a number of layers stacked upon the SAM: the water separating the SAM from the bilayer (central water), the adjacent lipid headgroups, the hydrophobic layer (inner and outer leaflet lipid chains) and the lipid headgroups in contact with the bulk solvent. The simultaneous altering of the thickness, roughness, SLD and solvation of all these model layers, within physically reasonable limits, allowed theoretical NR curves to be fitted to the experimentally-obtained ones (figures 5 and 6). An overall Chi-squared value obtained from the fitting software, together with the results of a bootstrapping error analysis on the parameter values obtained for each layer (run 100 times with 1000 iterations per run), were used to assess the closeness of the fits (table 4). In addition to obtain theoretical NR curves, fitting also allowed the construction of SLD profiles for each experimental treatment, allowing the relationship between the thickness, solvation and roughness of each layer in the model to be represented graphically (figures 5 and 6). For the purposes of making clear comparisons between the results of the various treatments, only the data obtained using D_2O and H_2O as bulk solvents are presented here since these were deemed to show the highest degree of contrast between the different components of the samples.
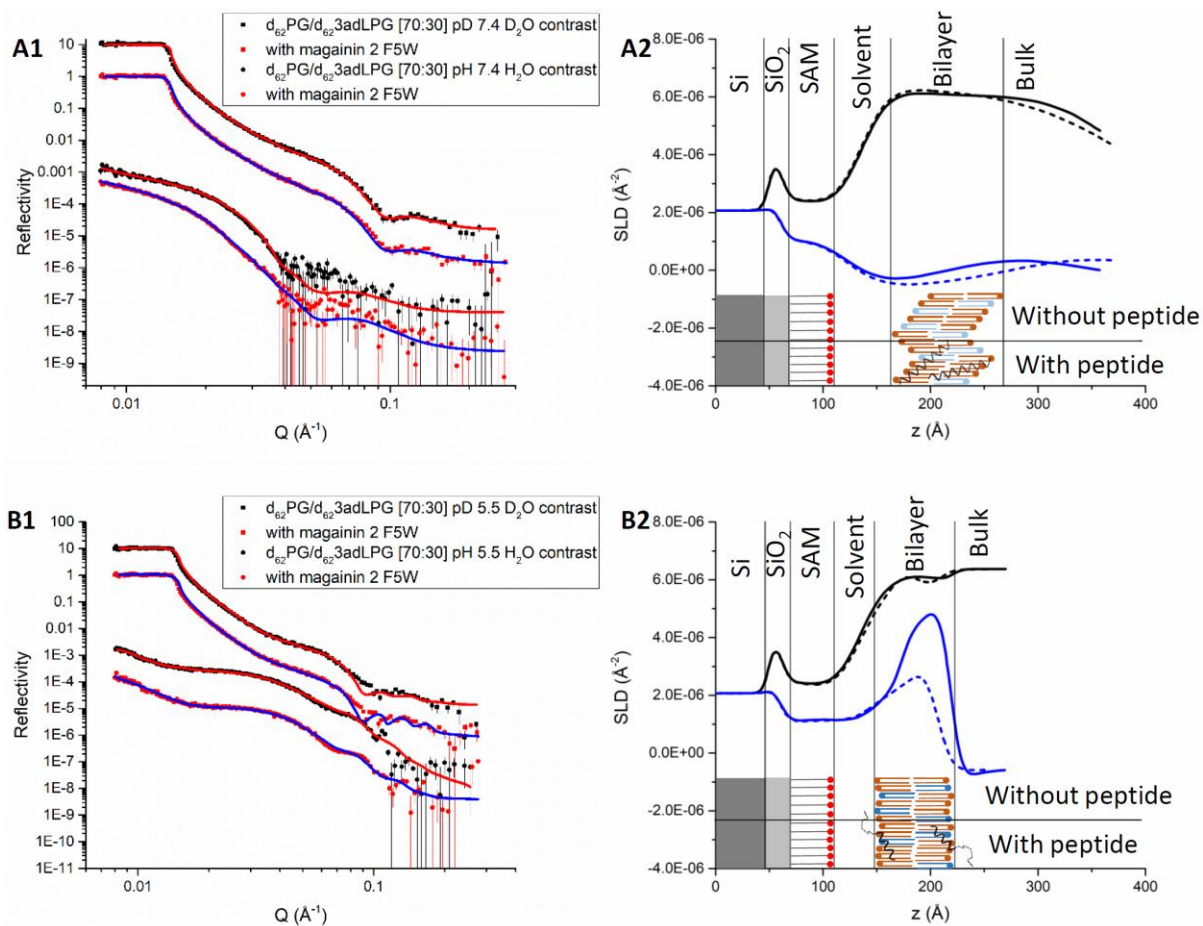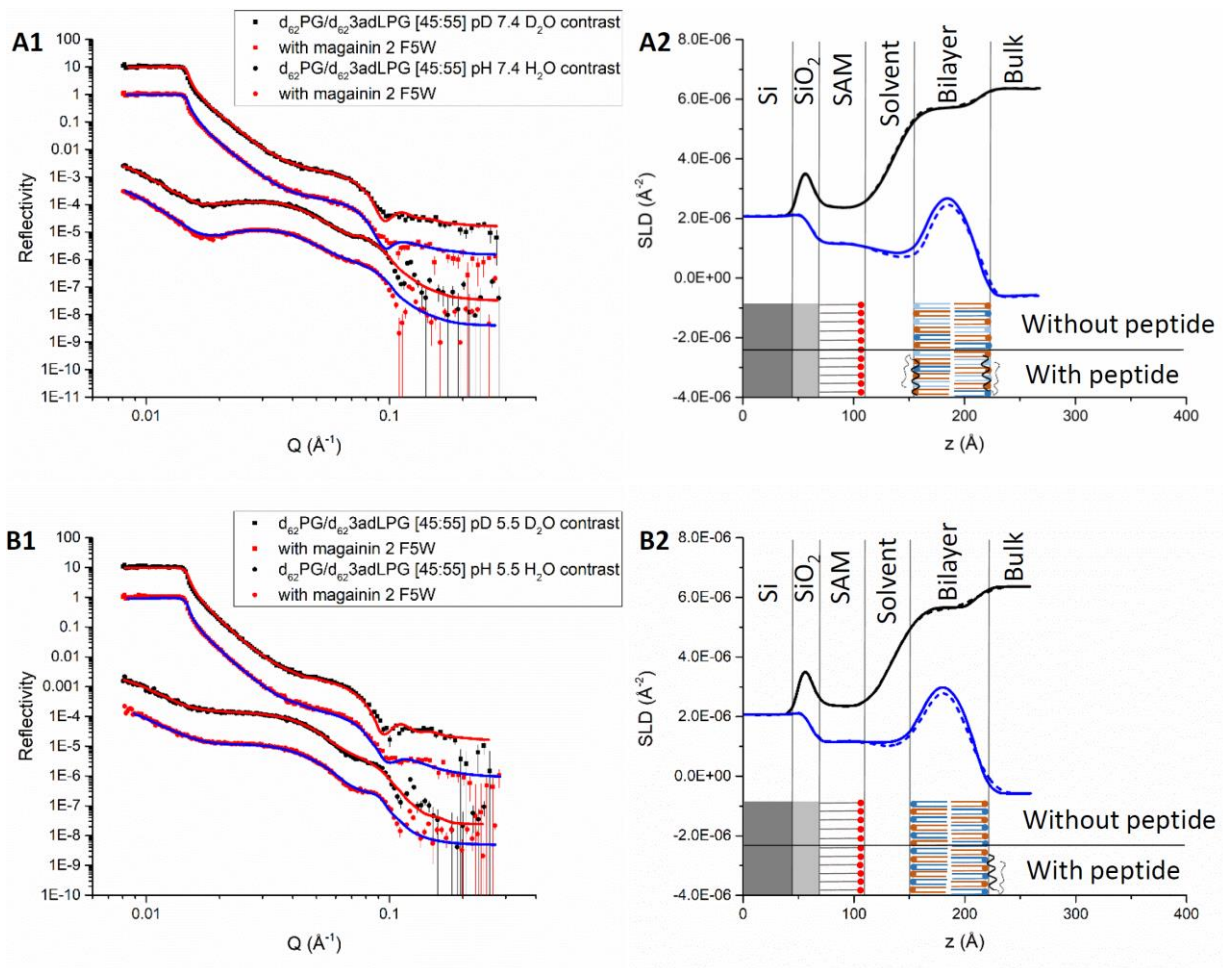
Figure 5. Fitted neutron reflectivity curves for $d_{62}DPPG/d_{62}DP3adLPG$ 7:3 at 55°C, in pH 7.4 buffer alone and with magainin F5W (A1) and in pH 5.5 buffer alone and with magainin F5W (B1). Together with their corresponding fit-derived SLD profiles (blue for H_2O and black for D_2O contrasts) and schematic interface cross-sections in pH 7.4 buffer alone (solid lines) and with magainin F5W (dashed lines) (A2) and in pH 5.5 buffer alone and with magainin F5W (B2).

The effects of both bulk solvent mild acidification and AMP challenge on the pH 7.4 culture mimetic $d_{62}PG/d_{62}3adLPG$ 7:3 floating bilayers (figure 5), are evident from the gross alterations in membrane structure implied by the observed changes in the fitted bilayer parameters, obtained from the reflectivity curves (table 4). The bilayers, as initially

characterized in bulk solvents at pH 7.4, appear to have been highly disordered. This is apparent from the absence of distinct SLD differences between the membrane layer and the bulk solvent (figure 5 A2), the large central water thickness (>100 Å), high degree of chain hydration (~26%) and high roughness (~23 Å). Taken in isolation these data could imply that the sample was of poor quality and did not adequately cover the surface of the SAM. However the lowering of the bulk pH to 5.5 induced significant changes whereby the separation between the SAM and the bilayer was reduced to 29 Å, the lipid chain hydration decreased to ~0.7 % (implying a very comprehensive SAM coverage) and the bilayer roughness was reduced to ~7.2 Å. Together with the significant differences between the SLD of the bilayer and those of the central water and bulk solvent (figure 5 B2), these changes imply that mild acidification of the membrane environment elicits a significant ordering effect upon the bilayers, even in the fluid phase. At pH 7.4, the d_{62}3adLPG would predominantly be in a zwitterionic form (pale blue lipids in figure 5 A2) whereby only the phosphate and ε amine groups were ionized. The lateral packing stress exerted by the presence of an excess of anionic d_{62}PG (brown lipids in figure 5 A2) in the sample, would thus be relaxed by an increase in bilayer undulation (hence the apparent disorder). At pH 5.5, however, when the d_{62}3adLPG was predominantly fully ionized (dark blue lipids in figure 5 B2), it would have been able to form neutral ion pairs or triplets (Duran, et al. 2016, Schmid, et al. 2018) with the d_{62}PG, thus reducing the lateral packing stress and stabilizing the bilayer.

After characterization of the d_{62}PG/d_{62}3adLPG 7:3 sample at pH 7.4 and then at pH 5.5, the AMP magainin 2 F5W was introduced into the sample at pH 7.4. The presence of the peptide appeared to increase the disorder within the membrane, as evidenced by the

increases in central water thickness, lipid chain hydration and bilayer roughness (table 4). The change in bilayer density, most noticeable from the decrease in hydrophobic chains thickness (from ~32 Å to ~26 Å) and SLD (from 6.73×10^{-6} Å^{-2} to 5.15×10^{-6} Å^{-2}), suggest the presence of peptide (SLD ~1×10^{-6} Å^{-2}) within this region of the sample (Ludtke, et al. 1995). Although decreasing the bulk pH to 5.5 elicits an ordering of the bilayer, as was observed in the peptide-free sample, the maintenance of a high chain hydration, suggests that some material had been lost form the floating bilayer as a result of peptide action at pH 7.4. The decreased hydrophobic chain SLD suggests that some magainin 2 F5W remained associated with this region, but with a lesser impact than at pH 7.4, since the hydrophobic layer was thicker than that produced by peptide interaction at neutral pH. Therefore, despite the apparent damage to the floating bilayer caused by the peptide at pH 7.4, the ordering of the peptide elicited by mild acidity appeared to decrease the degree of peptide partitioning.

Figure 6. Fitted neutron reflectivity curves for d_{62}DPPG/d_{62}DP3adLPG 45:55 at 55°C, in pH 7.4 buffer alone and with magainin F5W (A1) and in pH 5.5 buffer alone and with magainin F5W (B1). Together with their corresponding fit-derived SLD profiles (blue for H_2O and black for D_2O contrasts) and schematic interface cross-sections in pH 7.4 buffer alone (solid lines) and with magainin F5W (dashed lines) (A2) and in pH 5.5 buffer alone and with magainin F5W (B2).

For the pH 5.5 culture mimetic d_{62}PG/d_{62}3adLPG 45:55 floating bilayer (figure 6), the decrease in bulk pH from 7.4 to 5.5 has little appreciable effect on the ordering of the membrane, beyond a decrease in chain region hydration (table 4), which is a possible

indication of decreased undulation. Although any undulation present in the sample at pH 7.4 must take place over a long lateral distance, since the local roughness remains low (8 Å). The slight thickening of the headgroup region at pH 5.5 (by ~3 Å) and a concomitant small alteration in headgroup SLD, probably result from the association of d_{62}PG and d_{62}3adLPG headgroups as ion pair formation was promoted at the lower pH. The lipid chain hydration of the sample at pH 5.5 suggests that the floating bilayer achieved around 90% coverage of the SAM.

Challenge of the d_{62}PG/d_{62}3adLPG 45:55 floating bilayer with magainin 2 F5W at pH 7.4 induced small changes to the bilayer SLD profiles (figure 6 A2), which are mainly associated with the lipid headgroups, although the fit suggests there is an accompanying modest increase in chain hydration (table 4). The decrease in headgroup region SLD (from 4.93 $\times 10^{-6}$ Å^{-2} to 3.84 $\times 10^{-6}$ Å^{-2}), together with a small decrease in headgroup thickness and an increase in hydration, with no accompanying significant effect on these parameters in the hydrophobic region, suggest that peptide associated with the bilayer was localized in the headgroup region. With the lowering of the bulk pH to 5.5, the bilayer parameters revert to values very close to those obtained for the peptide free sample fits at the same pH (figure 6 B2). Thus, it seems that any peptide associated with the floating bilayer at pH 7.4, for the most part dissociated from it at pH 5.5. At the mildly acidic pH all of the d62 PG in the bilayer is most likely ion-paired to cationic d_{62}3adLPG and therefore unavailable for interaction with the peptide. Furthermore, the increased ordering of the bilayer, elicited by the formation of ion pairs between almost all of the lipids present, may also have contributed to the expulsion of the peptide and protection of the membrane against the destructive effects of magainin 2 F5W.

Table 4. Structural parameters for d$_{62}$DPPG/d$_{62}$DP3adLPG bilayers derived from the fitting of neutron reflectivity curves for samples studied at 55°C with (+) and without (-) magainin 2 F5W peptide in both pH 5.5 and 7.4 buffers (lipid/peptide molar ratio 50:1).

d$_{62}$PG/ d$_{62}$3adLPG	pH	Peptide	Layer	Thickness (Å)	SLD (×10^{-6} Å^{-2})	Hydration (%)	Roughness (Å)
70:30			Central water	118.8 ± 19.6		100	
	7.4	-	Headgroups	8.0 ± 1.3	1.89	53.9 ± 7.4	23.1 ± 14.8
			Chains	32.4 ± 3.4	6.73	26.4 ± 7.5	23.1 ± 14.8
			Central water	29.0 ± 5.6		100	
	5.5	-	Headgroups	8.1 ± 1.3	4.08	16.2 ± 3.6	7.2 ± 2.7
			Chains	31.4 ± 2.6	7.06	0.7 ± 0.4	7.2 ± 2.7
			Central water	154.8 ± 23.4		100	
	7.4	+	Headgroups	13.9 ± 3.7	1.62	60.9 ± 6.6	32.5 ± 18.4
			Chains	26.2 ± 1.7	5.15	38.6 ± 8.9	32.5 ± 18.4
			Central water	17.6 ± 2.4		100	
	5.5	+	Headgroups	12.9 ± 2.7	4.05	41.6 ± 7.3	10.9 ± 3.6
			Chains	28.4 ± 6.4	5.87	38.1 ± 7.4	10.9 ± 3.6
45:55			Central water	14.2 ± 2.3		100	
	7.4	-	Headgroups	14.3 ± 4.2	4.93	47.1 ± 5.1	8.0 ± 0.6
			Chains	33.1 ± 4.6	5.84	34.3 ± 6.7	8.0 ± 0.6
			Central water	18.5 ± 1.9		100	
	5.5	-	Headgroups	16.9 ± 4.1	4.62	26.4 ± 7.9	9.5 ± 3.5
			Chains	32.2 ± 4.6	5.50	8.7 ± 3.7	9.5 ± 3.5
			Central water	14.9 ± 2.6		100	
	7.4	+	Headgroups	12.8 ± 6.1	3.84	53.4 ± 7.2	8.0 ± 1.9
			Chains	32.0 ± 5.5	5.27	37.0 ± 5.1	8.0 ± 1.9
			Central water	16.8 ± 0.7		100	
	5.5	+	Headgroups	15.5 ± 3.3	4.58	28.0 ± 6.4	10.0 ± 1.5
			Chains	32.7 ± 3.9	5.46	11.7 ± 5.8	10.0 ± 1.5

4. Discussion

The staphylococcal regulatory pathway linking the detection of membrane stress by the two component system GraSR to the upregulation of the lysyl-transferase encoding *mprF* gene, and subsequent increased biosynthesis of lysylphosphatidylglycerol, has

been well characterised (Fedtke, et al. 2004, Otto 2009). An increased proportion of LPG in the outer leaflet of staphylococcal membranes has been linked to resistance to human AMPs (Kristian, et al. 2003, Mukhopadhyay, et al. 2007, Ernst and Peschel 2011, Slavetinsky, et al. 2017), AMPs produced by competing bacteria (Draper, et al. 2015), and the lipopetide antibiotic of last resort, daptomycin (Chen, et al. 2018, Ma, et al. 2018, Müller, et al. 2018). The mechanism of this resistance is suggested to be an LPG-mediated dampening of the predominantly anionic membrane charge, which attenuates AMP/lipopeptide affinity for their lipid bilayer target (Fedtke, et al. 2004, Jones, et al. 2008). Various biophysical studies using synthetic lipid vesicles have attempted to demonstrate this charge dampening mechanism, with somewhat equivocal results. Experiments using both labile (Danner, et al. 2008) synthetic native LPG and its chemically stable analogue LPE have shown that although they attenuate AMP-induced membrane lysis, significant amounts of peptide remained bound to the lipid bilayers (Kilelee, et al. 2010, Cox, et al. 2014, Khatib, et al. 2016). None of these studies, however, had considered the role of mild acidity as an activator of LPG-mediated membrane protection, through inducing increased LPG biosynthesis (Gould and Lennarz 1970), eliciting demonstrable attenuation of peptide binding (Rehal, et al. 2017) and thus significant resistance to AMPs in *S. aureus* (Walkenhorst, et al. 2013). In this study we have presented experimental evidence for the combined roles of environmental pH, membrane charge properties and order which place LPG in a central role against various cation-mediated membrane-active threats.

The efficacy of membrane-targeting defensins, lantibiotics or lipopeptide antibiotics is dependent upon the overall charge of the bacterial envelope, and specifically the

plasmalemma target (Staubitz, et al. 2004, Draper, et al. 2015, Kreutzberger, et al. 2017). Cell envelope charge dampening has been shown to coincide with an increased expression of *mprF* (and *dltABCD*) in *S. aureus* (Ma, et al. 2018), and the resultant increase in LPG biosynthesis has been shown to successfully resist membrane perturbation by an AMP, especially in mildly acidic conditions (Rehal, et al. 2017). What this study demonstrates for the first time, through the use of biomimetic models containing a chemically stable LPG analogue, is the extent to which both LPG content and pH influence the membrane defence mechanism. Our DPPG/DP3adLPG/TMCL [67:28:5] model of the MRSA ST239 TW lipid bilayer, when cultured at pH 7.4, is vulnerable to perturbation by our representative AMP magainin 2 F5W, in bulk systems at both pH 7.4 and 5.5. Not only does the model show that the peptide is able to adopt its active α-helical conformation with lipids in the fluid phase, but that the peptide can readily partition into more tightly packed lipid monolayers, at both pHs. Increasing the proportion of DP3adLPG to >50% in the pH 5.5 culture MRSA ST239 TW model prevents the formation of α-helix by the peptide at both pHs, but does not prevent monolayer partitioning, most notably at pH 7.4. These results may be explained by observing the effect of 3adLPG content on membrane charge under both conditions (Supplementary Material figure S1).

Although LPG content of >50 mol% is sufficient to neutralise model *S. aureus* bilayers, it is only when LPG becomes predominantly fully ionized at pH 5.5, that these bilayers become significantly cationic (and thus presumably peptide repulsing). These results were corroborated by the NR studies on the simplified PG/3adLPG fluid phase floating bilayers, where the combination of both higher 3adLPG content and lower pH were

required to facilitate full membrane protection from peptide binding and partitioning. In the bacterium itself even small amounts of LPG may elicit AMP protection, since these are likely transported via the activity of the floppase subunit of MprF to the outer leaflet (Slavetinsky, et al. 2017). The asymmetric distribution of the lipids created by the MprF floppase would therefore need to maintain a proportion of LPG above 50 mol% in order to guarantee the formation of an electrostatic barrier to AMPs, although this would certainly be achievable under the mildly acidic conditions which promote LPG biosynthesis (Rehal, et al. 2017).

In addition to the effects of membrane charge, recent studies have suggested that lipid-mediated *S. aureus* resistance to daptomycin is in part facilitated by decreased membrane fluidity or the presence of lipid domains with reduced fluidity (Müller, et al. 2016, Boudjemaa, et al. 2018). Indeed it has been postulated that LPG could have a role in the formation of membrane domains in bacteria (Slavetinsky, et al. 2017), an idea which is supported by our finding that fully-ionized LPG has a condensing effect on model *S. aureus* bilayers, through the formation of PG/LPG ion pairs (Duran, et al. 2016). Although it could be argued that the monolayer results do not adequately represent the effect of ion pairing in natural lipid bilayers because they were obtained in the gel phase, the NR data depicts a more biomimetic situation. The pH 7.4 culture mimetic PG/3adLPG 7:3 mixture shows a dramatic ordering effect on the fluid floating bilayer, brought about by ion pairing between the lipid headgroups under mildly acidic conditions. Theoretically 60 mol% of the lipids in this system could form discrete neutral ion pairs at pH 5.5, leaving sufficient free anionic PG to interact with magainin 2 F5W, facilitating the observed peptide partitioning. Indeed the binding of the peptide to PG

may well induce the sequestration of the anionic lipid into less ordered domains, similar to those observed upon daptomycin interaction with *S. aureus* membranes (Müller, et al. 2016). Increasing the 3adLPG content of the floating bilayer to >50 mol% sequesters all of the anionic lipid into ion pairs at pH 5.5 (leaving some excess 3adLPG) eliciting a near total inhibition of AMP interaction.

5. Conclusions

The growth of *S. aureus* in mildly acidic conditions, mimicking those encountered by the bacterium on the skin or respiratory epithelium, facilitates the increased biosynthesis of lysylphosphatidylglycerol (Rehal, et al. 2017). As this study on synthetic *S. aureus* lipid bilayers shows, increased LPG analogue at low pH elicits a high degree of membrane protection against disruption by the model host-defensive APM magainin 2 F5W, through the formation of PG/LPG ion pairs. With the emergence of clinical MRSA isolates which exhibit higher rates of LPG synthesis with consequently greater resistance to therapeutic lipopeptides (Chen, et al. 2018), the profile of lipid-mediated bacterial intrinsic resistance mechanisms is rising. This is important because MRSA strains such as the ST239 TW upon which the model systems in this study are based, are showing a tendency toward increased transmission and proliferation (Edgeworth, et al. 2007, Santosaningsih, et al. 2018). In theory these strains may be primed by their fitness with respect to surviving skin acidity, via increased LPG biosynthesis, thus proving better adapted to resist both innate defensive and therapeutic lipopeptides/peptides. For this reason, the LPG-mediated two-for-one mechanism for circumventing epithelial or dermal defences can be considered as

a virulence factor enabling MRSA to continue evolving towards colonizing ever more diverse epithelial environments. Thus, the LPG biosynthesis pathway may constitute an attractive target for antivirulence therapeutics, with a view to interrupting the vicious cycle of resistance evolution which threatens to disarm our defences against MRSA infections.

Competing interests

The authors declare that they have no conflicting interests.

Acknowledgements

Appendix A. Supplementary Material

References

[1] M.W. Hornef, S. Normark, B. Henriques-Normark, M. Rhen, Bacterial evasion of innate defense at epithelial linings, Chem Immunol Allergy, 86 (2005) 72-98.

[2] T. Nakatsuji, T.H. Chen, S. Narala, K.A. Chun, T. Yun, F. Shafiq, P.F. Kotol, A. Bouslimani, A.V. Melnik, H. Latif, Antimicrobials from human skin commensal bacteria protect against Staphylococcus aureus and are deficient in atopic dermatitis, Science translational medicine, 9 (2017) eaah4680.

[3] A. Hakansson, C. Orihuela, D. Bogaert, Bacterial-Host Interactions: Physiology and Pathophysiology of Respiratory Infection, Physiological reviews, 98 (2018) 781-811.

[4] H.F.L. Wertheim, D.C. Melles, M.C. Vos, W. van Leeuwen, A. van Belkum, H.A. Verbrugh, J.L. Nouwen, The role of nasal carriage in Staphylococcus aureus infections, The Lancet Infectious Diseases, 5 (2005) 751-762.

[5] N.N. Mishra, S.-J. Yang, A. Sawa, A. Rubio, C.C. Nast, M.R. Yeaman, A.S. Bayer, Analysis of Cell Membrane Characteristics of In Vitro-Selected Daptomycin-Resistant Strains of Methicillin-Resistant Staphylococcus aureus, Antimicrobial Agents and Chemotherapy, 53 (2009) 2312-2318.

[6] A.S. Bayer, N.N. Mishra, A.L. Cheung, A. Rubio, S.-J. Yang, Dysregulation of mprF and dltABCD expression among daptomycin-non-susceptible MRSA clinical isolates, Journal of Antimicrobial Chemotherapy, 71 (2016) 2100-2104.

[7] F.-J. Chen, T.-L. Lauderdale, C.-H. Lee, Y.-C. Hsu, I.-W. Huang, P.-C. Hsu, C.-S. Yang, Effect of a Point Mutation in mprF on Susceptibility to Daptomycin, Vancomycin, and Oxacillin in an MRSA Clinical Strain, Frontiers in microbiology, 9 (2018).

[8] M.N. Alekshun, S.B. Levy, Commensals upon us, Biochem Pharmacol, 71 (2006) 893-900.

[9] A.J. Dobson, J. Purves, W. Kamysz, J. Rolff, Comparing selection on S. aureus between antimicrobial peptides and common antibiotics, PloS one, 8 (2013) e76521.

[10] H. Roy, Tuning the Properties of the Bacterial Membrane with Aminoacylated Phosphatidylglycerol, Iubmb Life, 61 (2009) 940-953.

[11] J.F. Tocanne, P.H.J.T. Ververgaert, A.J. Verkleij, L.L.M. van Deenen, A monolayer and freeze-etching study of charged phospholipids I. Effects of ions and pH on the ionic properties of phosphatidylglycerol and lysylphosphatidylglycerol, Chemistry and Physics of Lipids, 12 (1974) 201-219.

[12] M. Li, D.J. Cha, Y. Lai, A.E. Villaruz, D.E. Sturdevant, M. Otto, The antimicrobial peptide-sensing system aps of Staphylococcus aureus, Mol Microbiol, 66 (2007) 1136-1147.

[13] A. Peschel, R.W. Jack, M. Otto, L.V. Collins, P. Staubitz, G. Nicholson, H. Kalbacher, W.F. Nieuwenhuizen, G. Jung, A. Tarkowski, Staphylococcus aureus resistance to human defensins and evasion of neutrophil killing via the novel virulence factor MprF is based on modification of membrane lipids with l-lysine, The Journal of experimental medicine, 193 (2001) 1067-1076.

[14] C.M. Ernst, A. Peschel, Broad-spectrum antimicrobial peptide resistance by MprF-mediated aminoacylation and flipping of phospholipids, Mol Microbiol, 80 (2011) 290-299.

[15] R.P. Rehal, H. Marbach, A.T.M. Hubbard, A.A. Sacranie, F. Sebastiani, G. Fragneto, R.D. Harvey, The influence of mild acidity on lysyl-phosphatidylglycerol biosynthesis and lipid membrane physico-chemical properties in methicillin-resistant Staphylococcus aureus, Chem Phys Lipids, 206 (2017) 60-70.

[16] E.M. El Mashak, J.F. Tocanne, A monolayer study of the adsorption of methyl-lysine at phosphatidylglycerol-water interfaces: A model for elucidating the conformation of the Lisylphosphatidylglycerol polar head, Journal of Colloid and Interface Science, 70 (1979) 56-66.

[17] E. Kilelee, A. Pokorny, M.R. Yeaman, A.S. Bayer, Lysyl-Phosphatidylglycerol Attenuates Membrane Perturbation Rather than Surface Association of the Cationic Antimicrobial Peptide 6W-RP-1 in a Model Membrane System: Implications for Daptomycin Resistance, Antimicrobial Agents and Chemotherapy, 54 (2010) 4476-4479.

[18] S. Danner, G. Pabst, K. Lohner, A. Hickel, Structure and thermotropic behavior of the Staphylococcus aureus lipid lysyl-dipalmitoylphosphatidylglycerol, Biophysical Journal, 94 (2008) 2150-2159.

[19] E. Cox, A. Michalak, S. Pagentine, P. Seaton, A. Pokorny, Lysylated phospholipids stabilize models of bacterial lipid bilayers and protect against antimicrobial peptides, Biochimica et Biophysica Acta (BBA)-Biomembranes, (2014).

[20] R.M. Gould, W.J. Lennarz, Metabolism of phosphatidylglycerol and lysyl phosphatidylglycerol in *Staphylococcus aureus*, J Bacteriol, 104 (1970) 1135 - 1144.

[21] P.D. Cotter, C. Hill, Surviving the acid test: Responses of Gram-positive bacteria to low pH, Microbiol Mol Biol R, 67 (2003) 429-+.

[22] N. Washington, R.J.C. Steele, S.J. Jackson, D. Bush, J. Mason, D.A. Gill, K. Pitt, D.A. Rawlins, Determination of baseline human nasal pH and the effect of intranasally administered buffers, International Journal of Pharmaceutics, 198 (2000) 139-146.

[23] S. Schreml, R.M. Szeimies, S. Karrer, J. Heinlin, M. Landthaler, P. Babilas, The impact of the pH value on skin integrity and cutaneous wound healing, Journal of the European Academy of Dermatology and Venereology, 24 (2010) 373-378.

[24] S.H. Collins, W.A. Hamilton, Magnitude of the protonmotive force in respiring Staphylococcus aureus and Escherichia coli, Journal of bacteriology, 126 (1976) 1224-1231.

[25] J.D. Edgeworth, G. Yadegarfar, S. Pathak, R. Batra, J.D. Cockfield, D. Wyncoll, R. Beale, J.A. Lindsay, An Outbreak in an Intensive Care Unit of a Strain of Methicillin-Resistant Staphylococcus aureus Sequence Type 239 Associated with an Increased Rate of Vascular Access Device—Related Bacteremia, Clinical Infectious Diseases, 44 (2007) 493-501.

[26] K. Matsuzaki, Y. Mitani, K.-y. Akada, O. Murase, S. Yoneyama, M. Zasloff, K. Miyajima, Mechanism of synergism between antimicrobial peptides magainin 2 and PGLa, Biochemistry, 37 (1998) 15144-15153.

[27] R. Maget-Dana, The monolayer technique: a potent tool for studying the interfacial properties of antimicrobial and membrane-lytic peptides and their interactions with lipid membranes, Biochimica et Biophysica Acta (BBA)-Biomembranes, 1462 (1999) 109-140.

[28] K. Matsuzaki, K.-i. Sugishita, N. Ishibe, M. Ueha, S. Nakata, K. Miyajima, R.M. Epand, Relationship of Membrane Curvature to the Formation of Pores by Magainin 2, Biochemistry, 37 (1998) 11856-11863.

[29] R. Rehal, A Physicochemical and Biophysical Investigation into the Role of Lysyl-Phosphatidylglycerol in the Membrane of Staphylococcus aureus under mild acidic conditions., in: Institute of Pharmaceutical Science, King's College London, London, 2014.

[30] C.M. Lok, Versatile Methods for Synthesis of Mixed-Acid 1,2-Diacylglycerols, Chemistry and Physics of Lipids, 22 (1978) 323-337.

[31] P.R.J. Gaffney, C.B. Reese, Synthesis of naturally occurring phosphatidylinositol 3, 4, 5-trisphosphate [PtdIns (3, 4, 5) P 3] and its diastereoisomers, Journal of the Chemical Society, Perkin Transactions 1, (2001) 192-205.

[32] R. Rehal, A Physicochemical and Biophysical Investigation Into the Role of Lysylphosphatidylglycerol in the Membrane of Staphylococcus Aureus Under Mild Acidic Conditions, in, King's College London, 2014.

[33] P. Dynarowicz-Łątka, K. Hąc-Wydro, Interactions between phosphatidylcholines and cholesterol in monolayers at the air/water interface, Colloids and Surfaces B: Biointerfaces, 37 (2004) 21-25.

[34] R. Bucki, J.J. Pastore, P. Randhawa, R. Vegners, D.J. Weiner, P.A. Janmey, Antibacterial activities of rhodamine B-conjugated gelsolin-derived peptides compared to those of the antimicrobial peptides cathelicidin LL37, magainin II, and melittin, Antimicrobial agents and chemotherapy, 48 (2004) 1526-1533.

[35] M.D. Lad, F. Birembaut, L.A. Clifton, R.A. Frazier, J.R.P. Webster, R.J. Green, Antimicrobial Peptide-Lipid Binding Interactions and Binding Selectivity, Biophysical Journal, 92 (2007) 3575-3586.

[36] D.J.J. Barnes, D. Chu, Introduction to modeling for biosciences, Springer, London, 2010.

[37] C. Wiedemann, P. Bellstedt, M. Görlach, CAPITO—a web server-based analysis and plotting tool for circular dichroism data, Bioinformatics, 29 (2013) 1750-1757.

[38] A.V. Hughes, J.R. Howse, A. Dabkowska, R.A.L. Jones, M.J. Lawrence, S.J. Roser, Floating lipid bilayers deposited on chemically grafted phosphatidylcholine surfaces, Langmuir, 24 (2008) 1989-1999.

[39] T. Miyoshi, S. Kato, Detailed analysis of the surface area and elasticity in the saturated 1, 2-diacylphosphatidylcholine/cholesterol binary monolayer system, Langmuir, 31 (2015) 9086-9096.

[40] M. Schmid, C. Wolk, J. Giselbrecht, K.L.A. Chan, R.D. Harvey, A combined FTIR and DSC study on the bilayer-stabilising effect of electrostatic interactions in ion paired lipids, Colloids Surf B Biointerfaces, 169 (2018) 298-304.

[41] A.T. Duran, H. Marbach, B. Rasul, K. Andrew Chan, R.D. Harvey, Fourier Transform Infrared Spectroscopy Detection of Lipid Ion-Pairing in the Staphylococcus aureus Plasma Membrane, The FASEB Journal, 30 (2016) 877.871-877.871.

[42] S. Ludtke, K. He, H. Huang, Membrane thinning caused by magainin 2, Biochemistry, 34 (1995) 16764-16769.

[43] I. Fedtke, F. Gotz, A. Peschel, Bacterial evasion of innate host defenses - the Staphylococcus aureus lesson, International Journal of Medical Microbiology, 294 (2004) 189-194.

[44] M. Otto, Bacterial Sensing of Antimicrobial Peptides, in: M.S.R. Collin (Ed.) Bacterial Sensing and Signaling, 2009, pp. 136-149.

[45] S.A. Kristian, M. Durr, J.A.G. Van Strijp, B. Neumeister, A. Peschel, MprF-mediated lysinylation of phospholipids in Staphylococcus aureus leads to protection against oxygen-independent neutrophil killing, Infect Immun, 71 (2003) 546-549.

[46] K. Mukhopadhyay, W. Whitmire, Y.Q. Xiong, J. Molden, T. Jones, A. Peschel, P. Staubitz, J. Adler-Moore, P.J. McNamara, R.A. Proctor, M.R. Yeaman, A.S. Bayer, In vitro susceptibility of Staphylococcus aureus to thrombin-induced platelet microbicidal protein-1 (tPMP-1) is influenced by cell membrane phospholipid composition and asymmetry, Microbiol-Sgm, 153 (2007) 1187-1197.

[47] C. Slavetinsky, S. Kuhn, A. Peschel, Bacterial aminoacyl phospholipids – Biosynthesis and role in basic cellular processes and pathogenicity, Biochimica et Biophysica Acta (BBA) - Molecular and Cell Biology of Lipids, 1862 (2017) 1310-1318.

[48] L.A. Draper, P.D. Cotter, C. Hill, R.P. Ross, Lantibiotic resistance, Microbiol Mol Biol R, 79 (2015) 171-191.

[49] Z. Ma, E. Lasek-Nesselquist, J. Lu, R. Schneider, R. Shah, G. Oliva, J. Pata, K. McDonough, M.P. Pai, W.E. Rose, Characterization of genetic changes associated with daptomycin nonsusceptibility in Staphylococcus aureus, PloS one, 13 (2018) e0198366.

[50] A. Müller, F. Grein, A. Otto, K. Gries, D. Orlov, V. Zarubaev, M. Girard, X. Sher, O. Shamova, T. Roemer, P. François, D. Becher, T. Schneider, H.-G. Sahl, Differential daptomycin resistance development in Staphylococcus aureus strains with active and mutated gra regulatory systems, International Journal of Medical Microbiology, 308 (2018) 335-348.

[51] T. Jones, M.R. Yeaman, G. Sakoulas, S.-J. Yang, R.A. Proctor, H.-G. Sahl, J. Schrenzel, Y.Q. Xiong, A.S. Bayer, Failures in clinical treatment of Staphylococcus aureus infection with daptomycin are associated with alterations in surface charge, membrane phospholipid asymmetry, and drug binding, Antimicrobial agents and chemotherapy, 52 (2008) 269-278.

[52] E. Cox, A. Michalak, S. Pagentine, P. Seaton, A. Pokorny, Lysylated phospholipids stabilize models of bacterial lipid bilayers and protect against antimicrobial peptides, Biochim Biophys Acta, 1838 (2014) 2198-2204.

[53] T.O. Khatib, H. Stevenson, M.R. Yeaman, A.S. Bayer, A. Pokorny, Binding of daptomycin to anionic lipid vesicles is reduced in the presence of lysyl-phosphatidylglycerol, Antimicrobial agents and chemotherapy, (2016) AAC. 00744-00716.

[54] W.F. Walkenhorst, J.W. Klein, P. Vo, W.C. Wimley, pH Dependence of microbe sterilization by cationic antimicrobial peptides, Antimicrob Agents Chemother, 57 (2013) 3312-3320.

[55] P. Staubitz, H. Neumann, T. Schneider, I. Wiedemann, A. Peschel, MprF-mediated biosynthesis of lysylphosphatidylglycerol, an important determinant in staphylococcal defensin resistance, Fems Microbiology Letters, 231 (2004) 67-71.

[56] M.A. Kreutzberger, A. Pokorny, P.F. Almeida, Daptomycin–Phosphatidylglycerol Domains in Lipid Membranes, Langmuir, 33 (2017) 13669-13679.

[57] A. Müller, M. Wenzel, H. Strahl, F. Grein, T.N. Saaki, B. Kohl, T. Siersma, J.E. Bandow, H.-G. Sahl, T. Schneider, Daptomycin inhibits cell envelope synthesis by interfering with fluid membrane microdomains, Proceedings of the National Academy of Sciences, 113 (2016) E7077-E7086.

[58] R. Boudjemaa, C. Cabriel, F. Dubois-Brissonnet, N. Bourg, G. Dupuis, A. Gruss, S. Lévêque-Fort, R. Briandet, M.-P. Fontaine-Aupart, K. Steenkeste, Impact of Bacterial Membrane Fatty Acid Composition on the Failure of Daptomycin To Kill Staphylococcus aureus, Antimicrobial Agents and Chemotherapy, 62 (2018) e00023-00018.

[59] D. Santosaningsih, S. Santoso, N. Setijowati, H.A. Rasyid, N.S. Budayanti, K. Suata, D.B. Widhyatmoko, P.B. Purwono, K. Kuntaman, D. Damayanti, C.R.S. Prakoeswa, M. Laurens, J.W.I. Nierop, G.L. Nanninga, N. Oudenes, M. Regt, S.V. Snijders, H.A. Verbrugh, J.A. Severin, Prevalence and characterisation of Staphylococcus aureus causing community-acquired skin and soft tissue infections on Java and Bali, Indonesia, Tropical Medicine & International Health, 23 (2018) 34-44.